N-glycosylation shields *Phytophthora sojae* apoplastic effector PsXEG1 from a specific host aspartic protease

Yeqiang Xia[a,b,c], Zhenchuan Ma[a,b,c], Min Qiu[a,b,c], Baodian Guo[a,b,c], Qi Zhang[a,b,c], Haibin Jiang[a,b,c], Baiyu Zhang[a,b,c], Yachun Lin[a,b,c], Mingrun Xuan[a,b,c], Liang Sun[a,b,c], Haidong Shu[a,b,c], Junhua Xiao[a,b,c], Wenwu Ye[a,b,c], Yan Wang[a,b,c], Yiming Wang[a,b,c], Suomeng Dong[a,b,c], Brett M. Tyler[d,e], and Yuanchao Wang[a,b,c,1,2]

[a]Department of Plant Pathology, Nanjing Agricultural University, 210095 Nanjing, China; [b]Key Laboratory of Integrated Management of Crop Diseases and Pests (Ministry of Education), College of Plant Protection, Nanjing Agricultural University, Nanjing 210095, China [c]The Key Laboratory of Plant Immunity, Nanjing Agricultural University, 210095 Nanjing, China; [d]Center for Genome Research and Biocomputing, Oregon State University, Corvallis, OR 97331; and [e]Department of Botany and Plant Pathology, Oregon State University, Corvallis, OR 97331

Edited by Sheng Yang He, Duke University, Durham, NC, and approved September 17, 2020 (received for review June 12, 2020)

Hosts and pathogens are engaged in a continuous evolutionary struggle for physiological dominance. A major site of this struggle is the apoplast. In *Phytophthora sojae*–soybean interactions, PsXEG1, a pathogen-secreted apoplastic endoglucanase, is a key focal point of this struggle, and the subject of two layers of host defense and pathogen counterdefense. Here, we show that N-glycosylation of PsXEG1 represents an additional layer of this coevolutionary struggle, protecting PsXEG1 against a host apoplastic aspartic protease, GmAP5, that specifically targets PsXEG1. This posttranslational modification also attenuated binding by the previously described host inhibitor, GmGIP1. N-glycosylation of PsXEG1 at N174 and N190 inhibited binding and degradation by GmAP5 and was essential for *PsXEG1*'s full virulence contribution, except in GmAP5-silenced soybeans. Silencing of GmAP5 reduced soybean resistance against WT *P. sojae* but not against *PsXEG1* deletion strains of *P. sojae*. The crucial role of N-glycosylation within the three layers of defense and counterdefense centered on PsXEG1 highlight the critical importance of this conserved apoplastic effector and its posttranslational modification in *Phytophthora*-host coevolutionary conflict.

apoplast | *P. sojae* | N-glycosylation | aspartic protease | immunity

Microbial plant pathogens have evolved a variety of strategies to attack plant hosts to cause disease (1, 2). Early interactions between plant pathogens and their hosts occur in the extracellular space (apoplast) (3), where many kinds of molecular interactions, including attacking enzymes and counteracting inhibitors from both sides, play an important role in determining the overall outcome of infection (4, 5). The struggle for physiological dominance in the apoplast engages multiple layers of defense and counterdefense between hosts and pathogens.

Phytophthora sojae, the agent of soybean (*Glycine max*) root and stem rot, causes substantial worldwide soybean production losses (6). Previously, we found that the apoplastic xyloglucan-specific endoglucanase PsXEG1 of *P. sojae* is subject to two layers of defense and counterdefense (7–9). Recognition of PsXEG1 by the soybean pattern recognition machinery can block *P. sojae* infection; however, the PsXEG1-triggered immune response is, in turn, suppressed by multiple intracellular effectors (7, 8). PsXEG1 is also targeted by a second defense layer, the apoplastic inhibitor protein GmGIP1, which binds to PsXEG1 to inhibit its enzyme activity and, thereby, reducing *P. sojae* virulence; however, PsXEG1 is protected by a paralogous decoy, PsXLP1, which has evolved to bind more tightly to GmGIP1 than PsXEG1 (8).

Here, we show that PsXEG1 is subject to an additional layer host defense. PsXEG1 is degraded by the soybean aspartic protease GmAP5. However, N-glycosylation acts as a shield to protect PsXEG1 from degradation by GmAP5, which has evolved to specifically target PsXEG1, constituting an additional layer of defense and counterdefense. N-glycosylation of PsXEG1 also attenuates the binding by the inhibitor GmGIP1. The decoy PsXLP1 binds more tightly to GmGIP1 than PsXEG1 due to its lack of glycosylation sites and escapes from GmAP5 degradation by a C-terminal deletion. The crucial role of N-glycosylation across multiple layers of defense and counterdefense centered on PsXEG1 highlights the importance of posttranslational modification of a pathogen virulence factor in tipping the balance of an arms race in this host–pathogen conflict.

Results

PsXEG1 Is Degraded in the Apoplast. Immunoblot analysis of PsXEG1 protein produced during *P. sojae* infection suggested degradation of this key effector (Fig. 1*A*). Two isoforms of PsXEG1 could be detected, of which the smaller form was much more sensitive to degradation than the larger form, suggesting that the larger form was posttranslationally modified (Fig. 1 *A*–*C*). The protein synthesis inhibitor cycloheximide (CHX) was used to assay PsXEG1-HA (hemagglutinin) stability in the apoplast of *Nicotiana benthamiana* leaves; the results showed that transiently expressed PsXEG1-HA was rapidly degraded after CHX blocked new protein synthesis (Fig. 1*B* and *SI*

Significance

The apoplastic space is the initial battlefield in plant–microbe interactions. However, the molecular mechanisms underlying how apoplastic immunity controls pathogen invasion is still largely unknown. Here, we show that soybean secretes an apoplastic aspartic protease, GmAP5, that binds to and degrades PsXEG1 to block its contribution to virulence. *Phytophthora sojae*, however, employs N-glycosylation as a shield to protect PsXEG1 from degradation by GmAP5. N-glycosylation of PsXEG1 also attenuates the binding by the inhibitor GmGIP1. Our result uncovers an additional layer of defense and counterdefense centered on PsXEG1, highlighting an example in which N-glycosylation of a pathogen virulence factor tips the balance of an arms race in host–pathogen conflicts.

Author contributions: Y.X., Z.M., and Yuanchao Wang designed research; Y.X., Z.M., M.Q., B.G., Q.Z., H.J., B.Z., Y.L., M.X., L.S., H.S., J.X., W.Y., S.D., B.M.T., and Yuanchao Wang performed research; Y.X., Z.M., M.Q., B.G., Q.Z., H.J., H.S., W.Y., Yan Wang, Yiming Wang, B.M.T., and Yuanchao Wang analyzed data; and Y.X., Z.M., M.Q., Yan Wang, Yiming Wang, S.D., B.M.T., and Yuanchao Wang wrote the paper.

The authors declare no competing interest.

This article is a PNAS Direct Submission.

[1]Present address: No.1 Weigang, Department of Plant Pathology, Nanjing Agricultural University, 210095 Nanjing, China.

[2]To whom correspondence may be addressed. Email: wangyc@njau.edu.cn.

This article contains supporting information online at https://www.pnas.org/lookup/suppl/doi:10.1073/pnas.2012149117/-/DCSupplemental.

First published October 20, 2020.

Appendix, Fig. S1). The smaller isoform of PsXEG1 was particularly sensitive to degradation. To further examine the degradation of PsXEG1 by soybean apoplastic proteins, we incubated PsXEG1 protein purified from *P. sojae* with soybean apoplast fluid (AF), in the presence of various protease inhibitors mixture (PIs) for 1 h at 25 °C in vitro. Again, the smaller isoform of PsXEG1 was sensitive to degradation. However, the degradation of PsXEG1 was substantially inhibited by the aspartic protease inhibitor Pepstatin A (Pep A) as well as by the PIs mix (Fig. 1*C*). This result suggested that the apoplastic aspartic protease(s) were involved in PsXEG1 degradation.

Soybean GmAP5 Degrades PsXEG1 and Confers Host Resistance Against *P. sojae*. The apoplast-localized PsXEG1 inhibitor, GmGIP1, is a nonactive aspartic protease-like protein (8, 10),which directly interacts with PsXEG1. To determine whether enzyme-active homolog(s) of GmGIP1 target PsXEG1 for degradation, genome-wide analysis was performed to identify GmGIP1 homologs as putative active aspartic proteases (Dataset S1). RNA sequencing showed that two of these homologs, Glyma.11G215200.1 and Glyma.03G200900.1, exhibited similar timing of transcript accumulation as PsXEG1, with a peak at ~0.5 h postinoculation (hpi) during early infection by *P. sojae* (Fig. 1*D* and *SI Appendix*, Fig. S2*A*). To test the interaction between PsXEG1 and these two protease candidates, we performed in planta coimmunoprecipitation (Co-IP) assays after transient coexpression of these proteins in *N. benthamiana* leaves, Gm02G148200, was used as a negative control (8). The Western blot showed that Glyma.11G215200.1, hereafter named GmAP5, as well as positive control GmGIP1 could bind to PsXEG1, while another protease Glyma.03G200900 and the negative control Gm02G148200 could not bind to PsXEG1. The Western blot also confirmed the degradation of PsXEG1 by GmAP5 but not by any of the other coexpressed soybean proteins (Fig. 1*E*). To test binding to GmAP5 while mitigating degradation by GmAP5, in vitro green fluorescence protein (GFP) pull-down assays were performed at 4 °C and at pH 7.5. The results confirmed that GmAP5 could associate with only the smaller isoform of PsXEG1 in vitro (*SI Appendix*, Fig. S3*A*). Furthermore, PsXEG1 mutations that abolished GmGIP1 binding, PsXEG1^{X1,2,3}, did not influence binding to GmAP5, suggesting that GmAP5 and GmGIP1 bind differently to PsXEG1 (*SI Appendix*, Fig. S3).

GmAP5 was confirmed to be present in the soybean apoplast during *P. sojae* infection using mass spectrometry (MS) (*SI Appendix*, Fig. S2*B*), consistent with its predicted signal peptide and the two conserved aspartic protease catalytic motifs (*SI Appendix*, Fig. S2*C*). GmAP5-GFP (green fluorescence) fusion proteins could also be detected in the apoplast when transiently expressed in *N. benthamiana* leaves (*SI Appendix*, Fig. S2 *D* and *E*). To address the contribution of GmAP5-mediated of degradation PsXEG1 to host resistance against *P. sojae*, we generated transgenic soybean hairy roots in which GmAP5 or mutant GmAP5$^{D115S\&S328A}$ was overexpressed or the *GmAP5* gene was silenced (*SI Appendix*, Fig. S4). Overexpression of GmAP5 in soybean hairy roots, but not of its inactive mutant, GmAP5$^{D115S\&S328A}$, enhanced soybean resistance against *P. sojae*, as measured both by oospore numbers (Fig. 1 *F* and *G* and *SI Appendix*, Fig. S4*C*) and biomass of *P. sojae* (Fig. 1*H*). In line with this, silencing of GmAP5 in hairy roots compromised soybean resistance against *P. sojae* (Fig. 1 *F–H* and *SI Appendix*, Fig. S4 *A* and *B*). Together, these results indicated that GmAP5 positively regulates soybean resistance against *P. sojae*, presumably due to PsXEG1 degradation.

PsXEG1 Undergoes Glycosylation In Vivo. As noted above (Fig. 1 *A* and *B*), two isoforms of PsXEG1 could be detected in *P. sojae*-secreted proteins, one with a size of ~34 kDa (black circle in Fig. 1*C*) and the other ~26 kDa, with different sensitivities to degradation. These two isoforms were also present in *P. sojae* transformants overexpressing PsXEG1 (*SI Appendix*, Fig. S5) and after transient expression in *N. benthamiana* leaves (Fig. 1 *B* and *E* and *SI Appendix*, Fig. S6 *A* and *B*). Treatment with peptide-*N*-glycosidases (PNGase) A or F reduced the ~34-kDa PsXEG1 isoform to ~26 kDa (Fig. 2*A* and *SI Appendix*, Fig. S6*C*). Endoglycosidase H (EndoH) produced a slight reduction while *O*-glycosidase produced no reduction (Fig. 2*A* and *SI Appendix*, Fig. S6*C*). Consistent with that observation, the larger isoform of PsXEG1 stained positively for glycosyl groups, whereas the smaller isoform and PNGase A-treated PsXEG1 did not (*SI Appendix*, Fig. S6*D*). In line with this, only the smaller isoform of PsXEG1 was detected when PsXEG1 was transiently expressed in *N. benthamiana* in the presence of the N-linked glycosylation inhibitor tunicamycin (TM) (Fig. 2*B*). These results demonstrated that the larger isoform represented N-glycosylated PsXEG1 while the smaller isoform represented unglycosylated PsXEG1.

To pinpoint the N-glycosylation sites, PNGases-treated PsXEG1 purified from the *P. sojae* overexpression transformant OT17 (*SI Appendix*, Fig. S5) was analyzed using nanoscale liquid chromatography-tandem MS (LC-MS/MS) (Fig. 2*C*). N174 and N190 are identified as potential glycosylation sites (Fig. 2*D*, *SI Appendix*, Figs. S7 and S8, and Dataset S2). Both N174 and N190 are located in the N-glycosylation NxS/T (Asn-x-Serine/Threonine) motifs that are evolutionarily conserved in XEG1 orthologs from different *Phytophthora* species (*SI Appendix*, Fig. S11 and Dataset S3). Alanine or glutamine substitutions have been used to mutate glycosylation motifs (11, 12). Homologous modeling predicted that these substitutions would not disturb the overall structure of PsXEG1 (*SI Appendix*, Fig. S9). Glutamine substitutions of N174 or N190 of PsXEG1 in *P. sojae* transformants resulted in reduced glycosylation compared with PsXEG1 (*SI Appendix*, Figs. S10 *A*, *B*, and *D*), while simultaneous mutation of both sites completely ablated N-glycosylation (*SI Appendix*, Fig. S10 *C* and *D*). Loss of the N-glycosylated isoform was also observed when PsXEG1$^{S176A\&S192A}$ and PsXEG1$^{N174A\&N190A}$ double mutants were transiently expressed in *N. benthamiana* (*SI Appendix*, Fig. S10*E*), confirming that both the N and S/T positions in the NxS/T motif were essential for PsXEG1 glycosylation. Together, the results indicated that PsXEG1 was exclusively N-glycosylated at N174 and N190.

N-Glycosylation Is Essential for the Full Virulence Function of PsXEG1. To investigate the role of N-glycosylation in the virulence contributions of PsXEG1, we performed homology-directed repair (HDR)-mediated replacement of *PsXEG1* in *P. sojae* with *PsXEG1$^{N174A\&N190A}$* using CRISPR/Cas9 (13) (Fig. 2*E* and *SI Appendix*, Fig. S12 *A* and *B*). Two independent transformants carrying homozygous *PsXEG1$^{N174A\&N190A}$* replacements, T91 and T192, showed no significant differences in growth in vitro compared to the WT *P. sojae* strain (Fig. 2*F* and *SI Appendix*, Fig. S12*C*). In addition, secretion of PsXEG1 and *PsXEG1* transcript levels appeared normal in the two transformants (*SI Appendix*, Fig. S13). However, both *PsXEG1$^{N174A\&N190A}$* mutant lines produced significantly smaller lesions on soybean hypocotyls (Fig. 2 *G* and *H*). Furthermore, a significant reduction was observed in genomic qPCR measurements of *P. sojae* biomass in hypocotyls infected by the two mutant lines (Fig. 2*I*). Together, these data demonstrated that the two N-glycosylation sites of PsXEG1 were required for its full contribution to *P. sojae* virulence. We previously showed that xyloglucanase activity is required for the virulence contribution of PsXEG1. In *SI Appendix*, Fig. S14*C*, we demonstrated by in vitro, xyloglucanase activity assays that N-glycosylation of PsXEG1 was not required for the enzymatic degradation of xyloglucan.

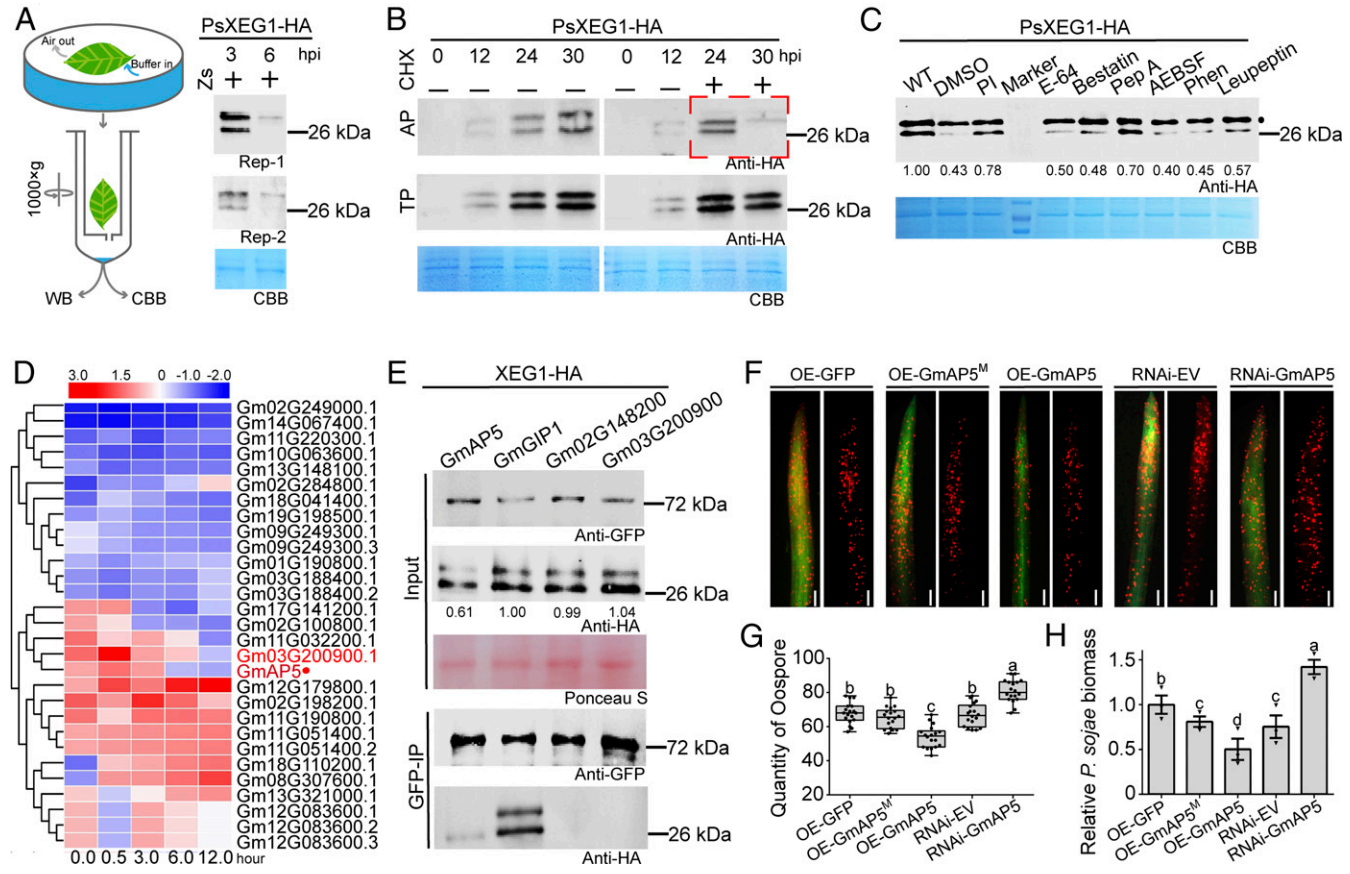

Fig. 1. Soybean GmAP5 binds with and degrades the PsXEG1, promoting resistance to *P. sojae*. (*A*) Immunoblot analysis of PsXEG1 protein produced during *P. sojae* infection. Soybean leaves were inoculated with zoospores of a *P. sojae* transformant ($T^{PsXEG1\text{-}HA}$) carrying an HA-tagged PsXEG1 gene, produced by CRISPR. At 3 and 6 hpi, the apoplastic fluid was extracted and concentrated using 3-kDa molecular mass centrifugal filter devices (Millipore) and subjected to immunoblot analysis using anti-HA antibodies and Coomassie Brilliant blue (CBB) staining. Rep-1 and Rep -2 indicate independent replicate experiments with similar results. (*B*) CHX assay of the stability of PsXEG1 in the apoplast. PsXEG1 was transiently expressed in *N. benthamiana* leaves by *Agrobacterium* (GV3101) infiltration. At 24 hpi, 10 μM CHX was infiltrated to stop protein synthesis (*Middle* with CHX, *Left* without CHX). At the same time (24 h after *Agrobacterium* inoculation), *P. parasitica* zoospores were sprayed onto the surface of the plant leaves at a concentration of 50/μL to stimulate a defensive environment in the apoplast. At 0 h, 12 h, 24 h, and 30 hpi after *Agrobacterium* inoculation, apoplastic fluid (*Top*; AF) or total protein (*Middle*, TP) were collected and analyzed by Western blotting with anti-HA antibody. CBB staining (*Bottom*) was used as a loading control. (*C*) Immunoblot analysis of PsXEG1 from *P. sojae* incubated with soybean apoplast fluid (AF) in combination with individual protease inhibitors for 1 h at 25 °C. Dimethyl sulfoxide (DMSO) was used as an inhibitor negative control. CBB staining was used to monitor the total amount of apoplastic protein loaded. This experiment was repeated three times with similar results. The apoplastic protein used in WT treatment (lane 1) was boiled to provide a degradation negative control. (*D*) Clustering analysis of soybean plant pepsin-like homologs based on RNA-seq data. RNA-seq data for each homolog were log-transformed by $y = \log_2(x + 1)$, and each infection time was standardized by $z = (y - \mu)/\sigma$ (where μ = the mean of the y values for each time and genes and σ = the SD of those values), then analyzed using TBtools Heatmap software with color scale. (*E*) Co-IP of C-terminal HA-tagged PsXEG1 and GFP-tagged Glyma.11G215200.1 (GmAP5) or Glyma.03G200900.1 transiently coexpressed in *N. benthamiana* leaves. GmGIP1 and Gm02G148200 were used as positive and negative controls, respectively. This experiment was repeated three times with similar results. (*F*) Oospore production at 36 hpi in transgenic hairy roots expressing GFP and either elevated GmAP5, $GmAP5^{M}$ = $GmAP5^{D115S\&S328A}$, or a GmAP5-silencing construct (GmAP5 RNAi or empty vehicle [EV] control) inoculated with *P. sojae* zoospores expressing RFP. Representative images by fluorescence microscope are shown. GmAP5 protein and transcript levels in hairy roots are shown in *SI Appendix*, Fig. S4. Three replicate experiments (each replicate contained six independent hairy roots) provided similar results. *Upper*, RFP + GFP; *Lower*, RFP. (Scale bars, 0.2 mm.) (*G* and *H*) *P. sojae* oospore quantities (*G*) and biomass (*H*) in infected roots. Three replicates of six roots each were used for each measurement (n = 18). Different letters represent significant differences, $P < 0.01$; Duncan's multiple range test. In *G*, bars represent medians and boxes the 25th and 75th percentiles, while in *H*, columns represent means normalized to OE-GFP and bars represent SEs.

GmAP5 Degrades Unglycosylated PsXEG1. *P. sojae* secretion assays with overexpression transformants further confirmed that N-glycosylation is not required for PsXEG1 secretion (*SI Appendix*, Fig. S14*A*). $PsXEG1^{N174A\&N190A}$ mutant protein could localize in the apoplast when it was transiently expressed in *N. benthamiana* leaves (*SI Appendix*, Fig. S14*B*). However, a protein synthesis inhibitor assay in *N. benthamiana* leaves showed that $PsXEG1^{N174A\&N190A}$-HA transiently expressed in the apoplast was rapidly degraded after CHX blocked the synthesis of new protein (Fig. 3*A*).

In an in vitro test using soybean apoplastic fluid mixed with purified PsXEG1 proteins, $PsXEG1^{N174Q\&N190Q}$ (produced in *P. sojae*) was rapidly degraded in the presence of apoplastic fluid, but this was substantially prevented by the aspartic protease inhibitor Pepstatin A (Fig. 3 *B* and *C*). Similar results were obtained with $PsXEG1^{N174A\&N190A}$ and $PsXEG1^{S176A\&S192A}$ produced in *N. benthamiana* (*SI Appendix*, Fig. S15). To confirm that the instability of these mutant proteins resulted from lack of glycosylation, deglycosylated PsXEG1 was also tested; it also was degraded when mixed with soybean apoplastic fluid, but not in the presence of Pepstatin A (Fig. 3*D* and *SI Appendix*, Fig. S15). Together, these results suggested that aspartic proteases were involved in the degradation of nonglycosylated PsXEG1 by the apoplastic fluid.

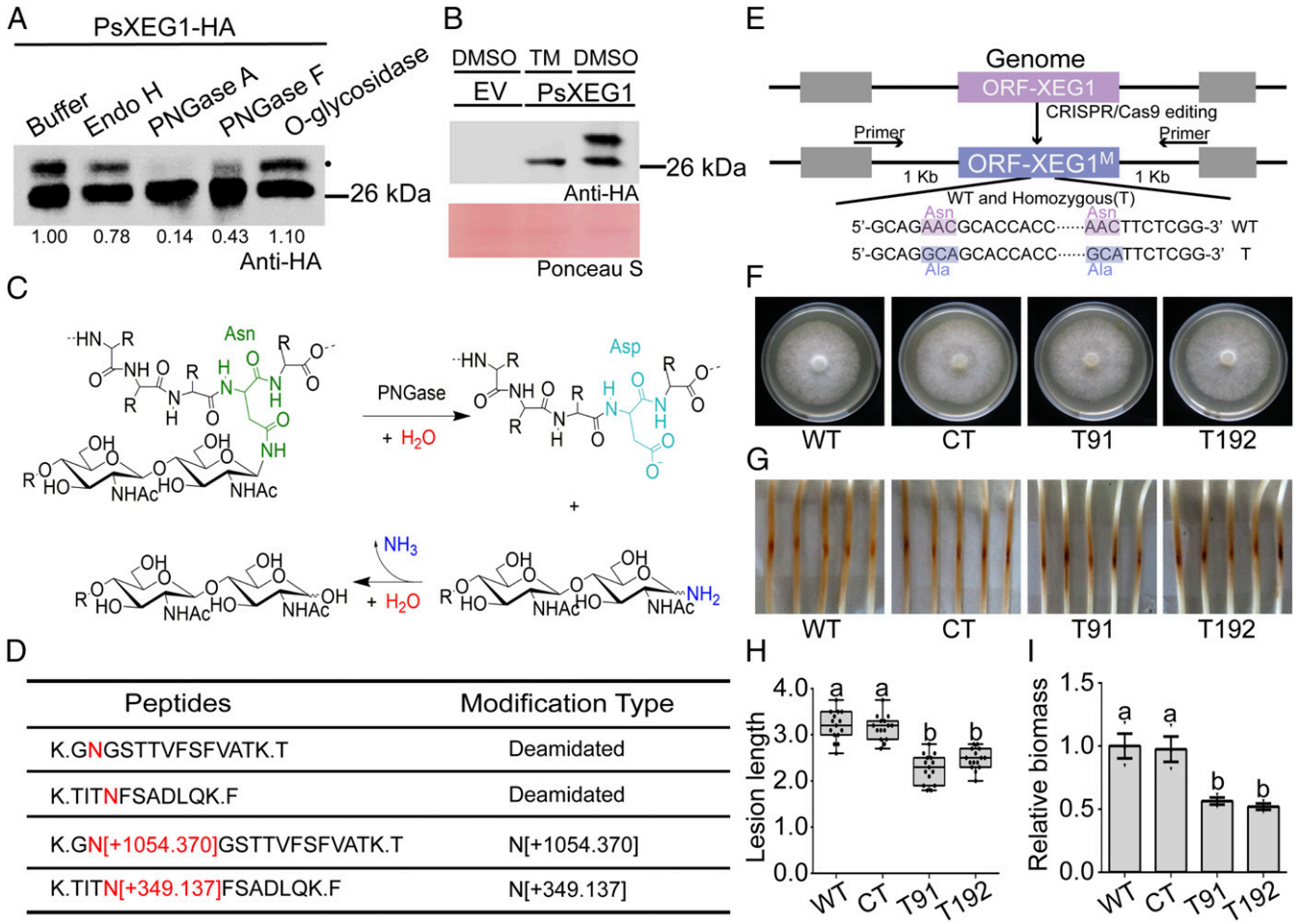

Fig. 2. PsXEG1 is N-glycosylated at N174 and N190, contributing to full *P. sojae* virulence. (*A*) De-glycosylation of PsXEG1 by N-glycosylases. PsXEG1 proteins from *P. sojae* OT17 were treated with EndoH, PNGase A, PNGase F, *O*-glycosidase, or a buffer control and analyzed by Western blotting using HA antibody. The numbers below the membrane indicate the band intensities of the glycosylated form of PsXEG1 (indicated by the black dot). (*B*) Glycosylation of PsXEG1 was inhibited by the N-glycosylation inhibitor TM in vivo. PsXEG1 with a C-terminal HA tag was transiently expressed in *N. benthamiana* leaves. After infiltration, leaf tissue was incubated for 12 h in the presence of 50 μg/mL TM or DMSO. Protein extracts were analyzed by Western blotting using anti-HA antibodies. Empty vector (EV) was used as a control for antibody specificity. Ponceau S staining indicates the total protein amount. (*C*) General reaction scheme for the enzymatic release of N-glycans by *PNGases*. (*D*) Identification of N-glycosylation sites and N-glycopeptides of PsXEG1 by LC-MS/MS. More details are shown in *SI Appendix*, Figs. S7 and S8. (*E*) Diagram of CRISPR HDR-mediated replacement of *PsXEG1* with the N-glycosylation mutant gene, $XEG1^{M}$ ($PsXEG1^{N174A\&N190A}$), in *P. sojae*. More details shown in *SI Appendix*, Fig. S12. (*F*) *PsXEG1* N-glycosylation site mutations in *P. sojae* transformants T91 and T192 had no effect on their growth. Representative images of colonies grown on V8 medium are shown. Three independent experiments produced similar results. (*G*) Infection phenotypes of *P. sojae* $PsXEG1^{N174A\&N190A}$ N-glycosylation mutants (T91 and T192) on etiolated soybean hypocotyls. Each hypocotyl was inoculated with ~100 zoospores and assessed 48 h later. Three independent experiments, each consisting of five hypocotyls per *P. sojae* strain, produced similar results. Representative images are shown. (*H*) Lesion lengths on hypocotyls produced by *P. sojae* WT, CT (control transformant lacking a *PsXEG1* mutation), and *PsXEG1* HDR mutants at 48 hpi. Three independent experiments, each consisting of five hypocotyls per *P. sojae* strain, were used for the measurements. Different letters represent significant differences, ($P < 0.01$; Duncan's multiple range test), bars represent medians, and boxes the 25th and 75th percentiles. (*I*) Relative biomass of PsXEG1 N-glycosylation mutants at 48 hpi, measured by genomic DNA qPCR. Three independent experiments, each consisting of five hypocotyls per *P. sojae* strain, were used for the measurements. Different letters indicate significant differences ($P < 0.01$; Duncan's multiple range test). Error bars indicate means with SEM.

To test whether GmAP5 could mediate $PsXEG1^{N174A\&N190A}$ degradation, we coexpressed GmAP5 and two other predicted aspartic proteases with $PsXEG1^{N174A\&N190A}$ in *N. benthamiana* leaves. Only GmAP5, but not the two other aspartic proteases, could accelerate degradation of apoplastic $PsXEG1^{N174A\&N190A}$ (Fig. 3*E*), and the degradation was inhibited by Pepstatin A in a dose-dependent manner (Fig. 3*F*). We also tested two enzyme-dead mutants of GmAP5, $GmAP5^{D115S\&S328A}$ and $GmAP5^{D115S\&Y178V}$, which carried mutations in the predicted active site. Compared with GmAP5, $GmAP5^{D115S\&S328A}$ and $GmAP5^{D115S\&Y176V}$ lost degradation activity toward $PsXEG1^{N174A\&N190A}$ (Fig. 3*G*). Together these results indicated that GmAP5 could target unglycosylated PsXEG1 for degradation in the apoplast.

GmAP5 Binds Specifically to Nonglycosylated PsXEG1. Next, we investigated the specific interaction between GmAP5 and PsXEG1 using GmAP5 proteins together with the inactive protease mutant $GmAP5^{D115S\&S328A}$ and the glycosylation mutant $PsXEG1^{N174A\&N190A}$, respectively. Using GmAP5-GFP fusion proteins purified from *N. benthamiana* leaves, mixed with $PsXEG1^{N174A\&N190A}$ purified from *Pichia pastoris*, we observed that $PsXEG1^{N174A\&N190A}$ could bind to $GmAP5^{D115S\&S328A}$ and also to the positive control, GmGIP1, but did not bind to the other two proteases (Fig. 4*A*). Additional GFP pull-down assays showed that Pepstatin A could reduce binding of GmAP5 to deglycosylated PsXEG1, suggesting that GmAP5 bound to PsXEG1 via its active center (*SI Appendix*, Fig. S16*A*).

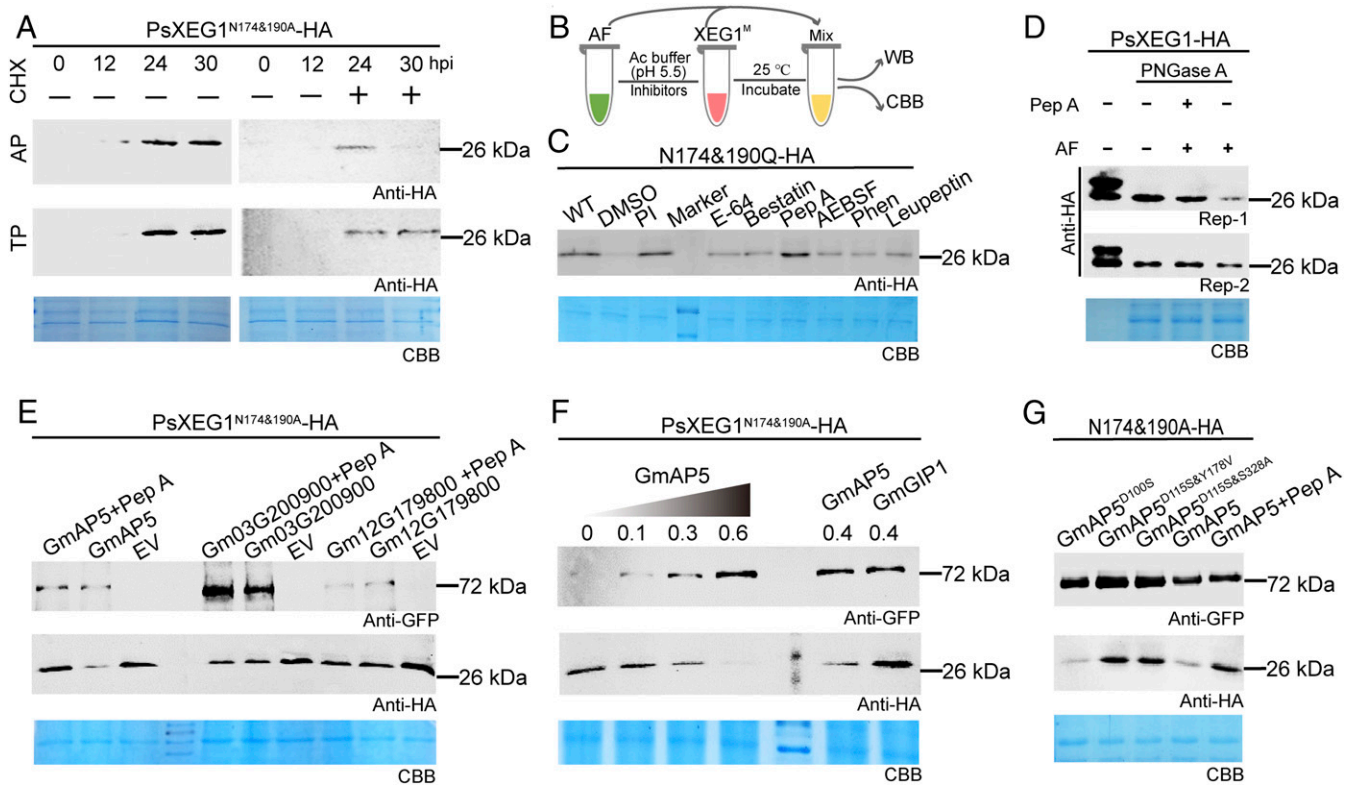

Fig. 3. Nonglycosylated PsXEG1 is unstable and degraded by GmAP5. (*A*) CHX assay of the stability of PsXEG1$^{N174A\&N190A}$ in the apoplast. PsXEG1$^{N174A\&N190A}$ was transiently expressed in *N. benthamiana* leaves by *Agrobacterium* (GV3101) infiltration. At 24 hpi, 10 μM CHX was infiltrated to stop protein synthesis (*Right* with CHX, *Left* without CHX). At the same time (24 h after *Agrobacterium* inoculation), *P. parasitica* zoospores were sprayed onto the surface of the plant leaves at a concentration of 50/μL to stimulate a defensive environment in the apoplast. At 0 h, 12 h, 24 h and 30 hpi after *Agrobacterium* inoculation, apoplastic fluid (*Upper*; AP) or total protein (*Lower*, TP) were collected and analyzed by Western blotting with anti-HA antibody. CBB staining was used as a loading control. This experiment was repeated three times with similar results. (*B*) Diagram showing the experimental approach used to assess the stability of PsXEG1 and its mutants for the experiment shown in *B*. AF was isolated from soybean leaves and a range of protease inhibitors was added. Samples were incubated with PsXEG1 protein purified from *P. sojae* overexpression transformants in the presence of sodium acetate buffer (50 mM NaAc pH 5.5) at 25 °C for 1 h, before analysis by Western blotting (WB) or CBB staining. CBB was used as a loading control for Western blot analysis of degradation to ensure that each experiment contained equal amounts of AF. (*C*) Immunoblot analysis of PsXEG1$^{N174Q\&N190Q}$ after incubation with soybean AF for 1 h at 25 °C in the presence of individual protease inhibitors (1,10-phenanthroline monohydrate, metalloprotease inhibitor; AEBSF, serine protease inhibitor; Bestatin, aminopeptidase inhibitor; E-64, cysteine protease inhibitor; Leupeptin, cysteine and serine protease inhibitor;Pepstatin A, acid aspartic protease inhibitor; PI, Plant Protease Inhibitor Mixture) as outlined in *A*. DMSO was used as an inhibitor negative control. CBB staining indicates the total amount of apoplastic protein loaded. This experiment was repeated three times with similar results. The apoplastic protein used in WT (lane 1) treatment was boiled as a degradation negative control. (*D*) Effects of protease inhibitor (Pepstatin A) on degradation of nonglycosylated PsXEG1 in the apoplast. PsXEG1 was deglycosylated by PNGase A for 24 h in NaAc buffer (pH 5.5). After 24 h, soybean apoplastic proteins with or without 1 mM Pepstatin A were added to the reaction, then 3 h later, Western blot analysis of the proteins was conducted using anti-HA antibodies. Coomassie Brilliant blue (CBB) was used to quantify the total apoplastic proteins as a loading control. Rep 1 and Rep 2 were two independent experiments. Untreated PsXEG1 protein was used as a control for deglycosylated reaction. (*E*) GmAP5, but not its paralogs, degrades PsXEG1$^{N174A\&N190A}$. Immunoblot analysis of C-terminal HA-fused PsXEG1$^{N174A\&N190A}$ transiently coexpressed with C-terminal GFP-fused GmAP5, Glyma.12G179800.1, or Glyma.03g200900.1 in *N. benthamiana* leaves for 36 h. The apoplastic proteins were harvested and incubated for 1 h at 25 °C with 1 mM pepstatin A or DMSO. CBB indicates the total protein loaded. This experiment was repeated three times with similar results. (*F*) PsXEG1 is degraded by GmAP5 in vivo in a dose-dependent manner. HA-tagged PsXEG1$^{N174A\&N190A}$ and GFP-tagged GmAP5 were coexpressed in *N. benthamiana* leaves. Different concentrations of *Agrobacterium* cells carrying *GmAP5* were used, as indicated by the OD numbers above the top. This experiment was repeated three times with similar results. GmGIP1 was used as a negative control. (*G*) Proteolysis of PsXEG1$^{N174A\&N190A}$ by GmAP5 proteins. C-terminal HA-fused PsXEG1$^{N174A\&N190A}$ and C-terminal GFP-fused GmAP5, GmAP5$^{D115S\&S328A}$, GmAP5$^{D115S\&Y178V}$, or GmAP5^{D100S} were transiently coexpressed in *N. benthamiana* leaves. After 36 h of expression, apoplastic fluid (AF) was harvested and incubated for 1 h at 25 °C. In one sample, 1 mM pepstatin A (Pep A) was directly added to the AF. DMSO was used as a negative control in all four other samples. Proteins were then analyzed by Western blotting with the indicated antibodies. CBB staining indicated the total amount of apoplastic protein loaded. This experiment was repeated three times with similar results.

Furthermore, using co-IP after transient coexpression in *N. benthamiana*, we observed that GmAP5$^{D115S\&S328A}$ and GmAP5 could only bind to nonglycosylated PsXEG1, but not to PsXLP1 or to a different glycohydrolase, PsGH6 (Fig. 4 *B* and *C*). In line with this, GmAP5 only degraded the unglycosylated form of PsXEG1, but could not degraded PsXLP1 or GH6 (Fig. 4 *B* and *C*). GmAP5 also failed to bind to three other PsXEG1 paralogs (*SI Appendix*, Fig. S16*B*). Since GmAP5 could not bind or degrade PsXLP1, which contains a C-terminal deletion compared to PsXEG1, we tested a comparable deletion mutant of PsXEG1, namely PsXEG1$^{\Delta 180–241}$. Neither GmAP5 nor GmAP5$^{D115S\&S328A}$ could bind PsXEG1$^{\Delta 180–241}$ (Fig. 4*C*). Together, these results indicate that GmAP5 is specialized for binding to and degrading PsXEG1, particularly the nonglycosylated form of PsXEG1. The results also show that PsXLP1, the decoy that protects PsXEG1 from GmGIP1, is resistant to GmAP5 degradation as a result of the C-terminal deletion.

N-Glycosylation Shields PsXEG1 from Degradation by GmAP5 during *P. sojae* Infection. To assess whether the specific interaction between GmAP5 and PsXEG1 occurred during *P. sojae* infection, we inoculated soybean hairy roots overexpressing or silencing GmAP5 with two *P. sojae* strains carrying mutations in their *PsXEG1* genes introduced by CRISPR, namely T91 (*PsXEG1*-$^{N174A\&N190A}$) and T3 (*PsXEG1*$^{\Delta}$) (8) (*SI Appendix*, Figs. S17 and S18). T91 infection was drastically reduced compared to the WT isolate when GmAP5 was overexpressed in the roots (Fig. 4 *D* and *F*). In contrast, the T91 transformant expressing unglycosylated PsXEG1 regained virulence on GmAP5-silenced transgenic plants (Fig. 4 *E* and *G*) However, the PsXEG1 knockout line, T3, caused similar infection of the soybean hairy roots irrespective of whether GmAP5 was silenced or overexpressed (Fig. 4 *D*–*G*). These results indicate that the role of GmAP5 in soybean defense depends on the presence of its target PsXEG1 and that N-glycosylation substantially shields PsXEG1 from GmAP5 attack during *P. sojae* infection.

The Binding Affinity of PsXEG1 to GmGIP1 Is Attenuated by N-Glycosylation. Glycosylation also attenuated PsXEG1 binding to GmGIP1, as indicated by the results of co-IP, pull-down, and biolayer interferometry experiments (*SI Appendix*, Fig. S19 *A*–*E*). GmAP5 belongs to a different plant pepsin-like aspartic protease clade from GmGIP1 (*SI Appendix*, Fig. S22*C*). GmAP5 contains the evolutionarily conserved aspartic protease catalytic domain, whereas GmGIP1 lacks a critical catalytic aspartate residue (8). In line with these sequence differences, GmAP5 is capable of degradation PsXEG1, while GmGIP1 failed to do so and acts by directly inhibiting PsXEG1 hydrolase activity (*SI Appendix*, Fig.

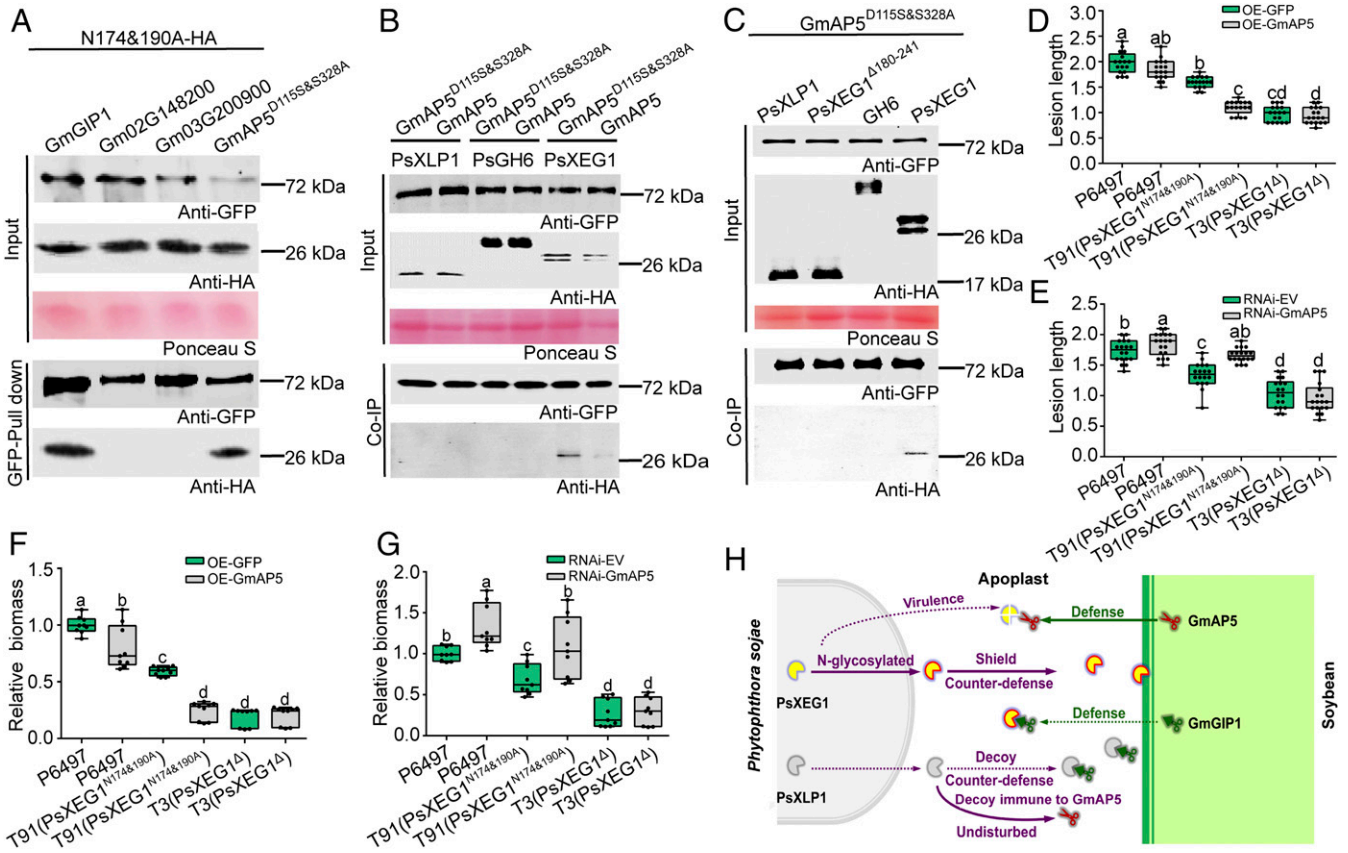

Fig. 4. N-glycosylation shields PsXEG1 from GmAP5 degradation in vitro and in vivo. (*A*) GmAP5$^{D115S\&S328A}$ bound to nonglycosylated PsXEG1 in vitro. GFP-tagged GmAP5$^{D115S\&S328A}$ or Gm03G200900 were expressed in *N. benthamiana* tissue, purified onto anti-GFP agarose-conjugated beads, then mixed with HA-His–tagged PsXEG1$^{N174A\&N190A}$ (produced in *P. pastoris*) in TNE buffer (10 mM Tris, 150 mM NaCl, 1 mM EDTA pH 7.5) at 4 °C for 1 h. After incubation and washing with TNE buffer, retained HA-His–tagged PsXEG1$^{N174A\&N190A}$ was detected with anti-HA antibodies. GmGIP1 was used as a positive control. Gm02G148200 was used as a negative control. This experiment was repeated three times with similar results. (*B*) Co-IP experiments showing the specificity of the GmAP5 interaction with and degradation of PsXEG1 in planta. C-terminal HA-tagged PsXEG1, PsXLP1, or PsGH6 (Ps_132587) were transiently coexpressed along with C-terminal GFP-tagged GmAP5 or GmAP5$^{D115S\&S328A}$ for 36 h in *N. benthamiana* leaves. Immunoprecipitates obtained from whole-cell extracts using anti-GFP trap beads were analyzed by immunoblotting with anti-HA and anti-GFP antibodies. This experiment was repeated three times with similar results. (*C*) Co-IP experiments showing that the PsXEG1 C terminus is an important determinant of the association of GmAP5 in planta. PsXEG1-HA, PsXEG1$^{\Delta 180-241}$-HA, or PsXLP1-HA were transiently coexpressed with GmAP5$^{D115S\&S328A}$-GFP transiently for 36 h in *N. benthamiana* leaves. PsGH6 (Ps_132587) was used as a negative control. Immunoprecipitates obtained from whole-cell extracts using anti-GFP trap beads were analyzed by immunoblotting with anti-HA and anti-GFP antibodies. This experiment was repeated three times with similar results. (*D*–*G*) Effects of GmAP5 overexpression (*D* and *F*) or silencing (*E* and *G*) on infection by *P. sojae* strains containing *PsXEG1* mutations. Soybean hairy roots expressing the indicated GmAP5 silencing or overexpression constructs were inoculated with *P. sojae* WT or mutant lines (T91, PsXEG1$^{N174A\&N190A}$; T3 PsXEG1$^{\Delta}$). The lesion lengths produced by *P. sojae* WT and PsXEG1 mutants at 36 hpi are shown on *D* and *E*. After 36 hpi, pathogen biomasss was measured by genomic DNA qPCR shown on *F* and *G*. OE-GFP, GFP alone overexpression control; OE-GmAP5, GmAP5-GFP fusion overexpression; RNAi-EV, empty vector silencing control; RNAi-GmAP5, GmAP5 silencing construct. Each experiment was replicated three times using 18 hairy roots from three different soybean cotyledons per biological replicate. Different letters represent significant differences ($P < 0.01$; Duncan's multiple range test). Bars represent medians and boxes the 25th and 75th percentiles. (*H*) Model of the integrated counterdefense by *P.* sojae against GmGIP1 and GmAP5 attacks on PsXEG1. N-glycosylation protects PsXEG1 against GmAP5 degradation and attenuates affinity to GmGIP1. The decoy, PsXLP1, binds more tightly to GmGIP1 than PsXEG1 and is protected from GmAP5 degradation by a C-terminal deletion.

S20 *A–D*). In addition, homology modeling and previous results showed that GmGIP1 mainly bound to the N terminus of PsXEG1, blocking the enzyme activity sites of PsXEG1 (8) (*SI Appendix*, Fig. S21 *A* and *B*). In contrast, GmAP5 binding requires the C terminus of PsXEG1 that is missing from PsXLP1 (which is immune to GmAP5) and that contains the two N-glycosylation sites (*SI Appendix*, Fig. S21 *A* and *B*). As a result, PsXLP1 can bind to GmGIP1 but not to GmAP5. Evolutionary analysis revealed that the split between GmAP5 and GmGIP1 is a very ancient event (*SI Appendix*, Figs. S22 *A*, *B*, and *D*). Thus, the two proteins have likely evolved independently to gain the ability to bind to PsXEG1 and, thus, they act on PsXEG1 virulence via different mechanisms.

Discussion

Hosts and pathogens are engaged in a continuous struggle for physiological dominance that drives the evolution and specialization of key defense and virulence proteins, respectively (4, 5). Until now, the role of posttranslational modifications of apoplastic effectors in this struggle have been poorly understood. Posttranslational modifications of intracellular effectors such as acylation, phosphorylation, ubiquitination, and proline isomerization have been described (14, 15), while, in bacterial pathogens, polymorphic glycans on flagella are a common strategy to evade host immunity mediated by pattern-recognition receptors (12). Another example is the *Magnaporthe oryzae* effector MoSlp1 that contains three N-glycosylation sites; Alg3-mediated N-glycosylation of all three sites is required to maintain protein stability and preserve the effector function of Slp1 (16). Defensive plant proteases have been characterized in the tomato-*Phytophthora infestans* pathosystem, where their importance to the host is underlined by the production of specific inhibitors by the pathogen (4, 17–20). However, the pathogen targets of those proteases are unknown. Here, we have shown that the aspartic protease GmAP5 plays a key role in defense against *P. sojae* by targeting the apoplastic effector PsXEG1. Overexpression of GmAP5 could reduce infection by WT *P. sojae* by 23% (Figs. 1 *F–H* and 4*F*) but had no effect against a *P. sojae* strain lacking PsXEG1 (Fig. 4*F*), indicating that the defense role of GmAP5 was focused on this single *P. sojae* apoplastic effector. N-glycosylation of PsXEG1 provided substantial protection against GmAP5 in vitro and during infection; N-glycosylation mutants of *PsXEG1* had 35% reduced virulence, but virulence was restored when *GmAP5* was silenced (Fig. 4 *D* and *E*). We previously showed that two layers of defense and counterdefense are focused on PsXEG1, one centered on recognition of PsXEG1 by pattern-recognition receptors (7–9) and the second centered on the host inhibitor protein GmGIP1 (8). The interplay between GmAP5 attack and N-glycosylation of PsXEG1 represents an additional layer of defense and counterdefense centered on this conserved apoplastic effector, in which N-glycosylation is a key player in the host–pathogen arms race (Fig. 4*H*). N-glycosylation also integrates with PsXLP1-mediated counterdefense against GmGIP1; N-glycosylation attenuates the affinity of PsXEG1 to GmGIP1 (*SI Appendix*, Fig. S19), while PsXLP1 binds more tightly to GmGIP1 than PsXEG1 due to its lack of glycosylation and is protected from GmAP5 degradation by a C-terminal deletion relative to PsXEG1(Fig. 4 *C* and *H*). We do not know if glycosylation affects recognition of PsXEG1 by the plant immune system (7).

Interestingly, GmAP5 belongs to a different pepsin-like plant clade than GmGIP1 (*SI Appendix*, Fig. S22*C*). GmAP5 contains the evolutionarily conserved aspartic protease catalytic domain, whereas GmGIP1 lacks a critical catalytic aspartate residue (8). The split between GmAP5 and GmGIP1 is very ancient (*SI Appendix*, Fig. S22*B*). Thus, the two proteins have independently evolved the ability to bind PsXEG1. Unlike GmGIP1, GmAP5 could not directly inhibit the enzymatic activity of PsXEG1 but degraded of PsXEG1 in the apoplast, indicating its primary defense strategy is PsXEG1 degradation rather than inhibition (Fig. 4*H*). The substantial differences in sequences and binding region to PsXEG1 between GmGIP1 and GmAP5 thus reflect the different defense strategies that they have evolved to provide (*SI Appendix*, Figs. S21 and S22). The unexpectedly narrow specificity of GmAP5 toward PsXEG1 may reflect not only the importance of PsXEG1 to the pathogen, but also a need of the plant to avoid degradation of its own apoplastic defense proteins. It will be of interest in the future to determine how many host apoplastic proteases target specific families of pathogen apoplastic effectors and to investigate the functions of the peptides released from pathogen apoplastic effectors by plant proteases in plant immunity.

Materials and Methods

RNA-Sequencing Experiments. Transcript level data for *PsXEG1*, and *GmAP5* and *GmAP5* homologs were obtained from previously published RNA-sequencing (seq) data (National Center for Biotechnology Information [NCBI] Sequence Read Archive (SRA) accession no. SRP073278) (21) and are listed in sheet 2 of Dataset S1. In that experiment, total RNA was extracted from *P. sojae* P6497 zoospore-infected susceptible soybean (Williams) roots at 0.5, 3, 6, 12 hpi.

Microbial Cultures. The *P. sojae* strains (P6497 and transformants) were maintained on 10% vegetable (V8) juice medium at 25 °C in the dark (9). *P. sojae* mycelia and zoospores were prepared as previously described (8).

***P. sojae* Transformation.** Homologous gene replacement in *P. sojae* was performed using the CRISPR/Cas9 system as previously described (13). *P. sojae* overexpression transformants were generated using polyethylene glycol-mediated protoplast transformation as previously described (22).

Transgenic Hairy Root Production from Soybean Cotyledons. Soybean (Williams cultivar) seeds were surface-sterilized and germinated as previously described (23). Soybean cotyledons were removed from 10-d-old seedlings grown in vermiculite. Cotyledons were harvested at day 7 by gently twisting them off the hypocotyl. Only unblemished cotyledons were employed for all protocols. Individual cotyledons were surface sterilized by wiping with an alcohol swab soaked in 70% ethanol. The alcohol swab was wrung out slightly before use, so that it was wet but not dripping. The surface-sterilized cotyledon was then cut by making a small, roughly circular (0.4-cm diameter) cut about 0.3 cm from the petiole end of the cotyledon to inoculate with *Agrobacterium rhizogenes* cell suspensions (24, 25). Before inoculation, the cells were centrifuged at 2,500 × *g* in a tabletop centrifuge for 20 min or until a relatively tight pellet of the bacteria was obtained. The K599 pellets were drained briefly and then gently resuspended in 10 mM $MgCl_2$ to a final OD_{600} of ∼0.4 for inoculation of cotyledon tissues as previously described (25). Inoculated cotyledons were placed in sterile Petri dishes containing MS medium and incubated in a growth chamber at 22 °C with a 16-h photoperiod. Hairy roots were monitored for green fluorescence production over a period of 4 wk. To monitor expression in hairy roots, total proteins were extracted from transgenic hairy roots exhibiting green fluorescence followed by immunoblotting. For silencing in hairy roots, the transcript levels of the targeted gene and its closest paralogs were measured in fluorescent green hairy roots using qRT-PCR to assess silencing efficiency

Multiple Sequence Alignment. All of the PsXEG1 sequences were obtained from the NCBI *P. sojae* database v3.0. The sequence search was limited to full-length sequences. The protein sequences were aligned using ClustalW and viewed using MEGA 4 (www.megasoftware.net).

Preparation and Purification of PsXEG1 Protein from *P. sojae*. To produce large quantities of secreted proteins, *P. sojae* strain OT17, containing a transgene consisting of a PsXEG1-HA-His_6 Tag fusion construct driven by the HAM34 promoter, was cultured in 1 L of synthetic liquid medium (0.5 g of KH_2PO_4, 0.5 g of Yeast extract, 0.25 g of $MgSO_4{\cdot}7H_2O$, 0.001 g of thiamine, 25 g of Glucose, 1 g of asparagine, 0.01 g of β-Sitosterol, made up to 1 L with Milli-Q-filtered H_2O) at 25 °C. After 10 d, the culture supernatant was collected and clarified by filtration through a 0.22-μm polyvinylidene fluoride membrane (Millipore). The proteins were precipitated overnight at 0 °C by adding 70 g of $(NH_4)_2SO_4$ per 100 mL of culture filtrate. The precipitate was

collected by centrifugation at 12,000 × *g* for 20 min at 4 °C and then resuspended in buffer A (50 mM NaH_2PO_4, 300 mM NaCl, and 10 mM imidazole). The resuspended proteins were purified by gel affinity chromatography with HisTrap HP on the ÄKTA system (GE Healthcare).

***Agrobacterium* and Protein Infiltration Assays.** *Agrobacterium*-mediated transient expression was performed as described (26). Plasmid constructs were introduced into *Agrobacterium tumefaciens* strain GV3101. After culturing for 36 h in liquid Luria-Bertani (LB) medium at 28 °C, bacterial cells were harvested by centrifugation and resuspended in infiltration medium (10 mM MES, 10 mM $MgCl_2$, 150 μM acetosyringone, pH 5.6). The optical densities of the cell suspensions in infiltration medium were adjusted to $OD_{600} = 0.4$ (final concentration for each strain in a mixture). Then, the cells were incubated for 2 h at room temperature before infiltration into leaves of 4-wk-old *N. benthamiana* plants. *N. benthamiana* leaves were harvested for protein extraction 36 h after infiltration, and apoplastic fluid from agroinfiltrated leaves was isolated as described previously (7, 27, 28). The apoplastic fluid was filter-sterilized (0.22-μm filters) and used immediately or stored at –80 °C.

Expression and Purification of Recombinant PsXEG1 and Mutant Protein in *P. pastoris*. *P. pastoris* KM71H (MutS) (Invitrogen) was used as the expression host. Cultures were maintained on yeast extract-peptone-dextrose medium. Buffered glycerol-complex medium was used for growth and buffered methanol-complex medium for induction, both at pH 6.5 (EasySelect Pichia Expression Kit; Invitrogen). *P. pastoris* transformants containing a His_6 fusion gene were screened for protein induction in 24-well plates as described previously (9). Protein expression was induced according to the manufacturer's instructions. The recombinant protein from the culture supernatant was purified by affinity chromatography using HisTrap HP with the ÄKTA system.

Prediction of Glycosylation Sites. The NetNGlyc 1.0 Server, which examines the amino acid sequence context of Asn-Xaa-Ser/Thr motifs (where Xaa is any amino acid except Pro) was used to predict potential N-glycosylation sites in PsXEG1 (Gupta, R. Prediction of N-glycosylation Sites in Human Proteins, www.cbs.dtu.dk/services/NetNGlyc).

Glycosylation Analysis of PsXEG1. To confirm the glycosylation of PsXEG1 protein, we treated PsXEG1 protein with PNGase A, PNGase F, EndoH, or *O*-glycosidase (New England Biolabs) at 37 °C for 1 h, as described by the manufacturer. Reaction buffer (50 mM Tris·HCl pH 7.5, 10% Nonidet P-40, 0.5% sodium dodecyl sulfate, 40 mM dithiothreitol) was used as a control. To stain purified PsXEG1 protein for glycosylation, we used the fuschin sulfite-based Glycoprotein Staining Kit (Pierce/Thermo Scientific) as described by the manufacturer.

Identification of N-Glycosylation Sites and N-Glycopeptides by LC-MS/MS. PsXEG1 proteins were treated with PNGases F and A for LC-MS/MS analysis. In-gel trypsin digestion was performed according to standard protocols. The dried peptides were redissolved in solvent A (0.1% formic acid in water), separated by nano-LC (Easy nLC 1200), and analyzed using a Thermo Q Exactive mass spectrometer. A typical gradient was run for 0–40 min from 5 to 30% solvent B (0.1% formic acid in acetonitrile), 40–45 min from 30 to 60% solvent B, 45–48 min from 60 to 80% solvent B, 45–48 min from 60 to 80% solvent B, 48–56 min in 80% solvent B, 56–58 min from 80 to 5% solvent B, and 58–65 min in 5% solvent B. The flow rate was set at 600 nL/min on an Acclaim PepMap 100, C18 (Thermo Scientific). Peptides were identified using the Mascot search engine and the UniProtKB protein database in Protein Discoverer 1.2. The results were filtered to maintain a protein false discovery rate of <1%.

Protein disulfide bonds of the samples were reduced for 40 min with 5 mM DTT at room temperature and alkylated for 40 min with 15 mM iodoacetamide in the dark. The alkylated protein samples were digested overnight at 37 °C with trypsin in a 1:50 enzyme-to-substrate ratio (Promega, V5113). Following digestion, the peptide mixtures were acidified with trifluoroacetic acid to 1% and desalted using a homemade C18 tip. Finally, the desalted peptide samples were dried in a vacuum concentrator, which produced purified peptide samples for analysis with a nanoLC-MS/MS Easy-nLC 1000 (Thermo Fisher Scientific). The MS and MS/MS data were acquired under higher energy collision-induced dissociation (HCD) product ion triggered collision-induced dissociation (CID) mode, using a 3-s top speed mode cycle time. The resulting HCD MS^2 data were searched for tentative glycopeptide matches using Byonic v. 2.9.38 (Protein Metrics) with the following parameters: protein modifications, carbamidomethylation (C) (fixed) and oxidation (M) (variable); enzyme specificity, trypsin; maximum missed cleavages, 2; precursor ion mass tolerance, 10 ppm; and MS/MS tolerance, 0.6 Da. The returned positive glycopeptide hits were then validated manually by considering both the HCD and CID MS^2 results.

Inhibitors Used for Measurement of PsXEG1 Stability. CHX was used to inhibit protein synthesis in plant cells. One millimolar cysteine protease inhibitor E-64 ((1*S*,2*S*)-2-(((*S*)-1-((4-Guanidinobutyl)amino)-4-methyl-1-oxopentan-2-yl)carbamoyl) cyclopropane carboxylic acid; Product Code E3132), 1 mM serine protease inhibitor AEBSF (4-(2-Aminoethyl) benzene-sulfonyl fluoride hydrochloride; Product Code A8456), 0.5 mM metallo-aminopeptidase inhibitor Bestatin (Product Code B8385), 1 mM acid protease inhibitor Pepstatin A (Product Code P4265), 1 mM metalloprotease inhibitor 1,10-phenanthroline monohydrate (Product Code P9375) and Plant Protease Inhibitor Mixture (Product code P9599; PI; contains AEBSF, Bestatin, E-64, Leupeptin, Pepstatin A, 1,10-Phenanthroline) were purchased from Sigma-Aldrich and used to inhibit proteolysis.

DNS Assays Used to Measure the Relative Enzyme Activity of XEG1. Xyloglucan (Megazyme) (1 μg/μL) solution in Na-acetate buffer (0.05 M, pH 5.5) was mixed with 2 μg of enzyme made up to 300 μL with Milli-Q-filtered H_2O. The reaction was incubated for 30 min at 42 °C. Then, adding 200 μL of DNS solution (6.4 g of 3,5-Dinitrosalicylic acid, 21.0 g of sodium hydroxide, 185.0 g of seignette salt, 5.0 g of Phenol, 5.0 g of sodium sulfite; all of the reagents were dissolved in 1 L of distilled water) incubated at 100 °C on a water bath for 5 min. The plate was cooled, and the absorbance at 540 nm was measured using a SpectraMax M5 microplate reader.

***P. sojae* Virulence Assays on Soybean Seedlings.** The virulence phenotypes of *P. sojae* WT and transformant strains were determined by inoculation of the hypocotyls of etiolated soybean seedlings. Approximately 100 zoospores of each strain were inoculated onto the hypocotyls of 3-d-old etiolated soybean seedlings (Williams cultivar). The inoculated hypocotyls were maintained in the dark at 25 °C before assessing infection. Disease symptoms were scored 48 h after infection. Each experiment was repeated for three times using total 15 hypocotyls (5 hypocotyls per experimental replicate).

For *P. sojae* hairy root infection assays, soybean hairy roots that were identical in morphology were removed from the cotyledons and inoculated with *P. sojae* WT (P6497) or mutant mycelia grown on V8 plates for 5 d. *P. sojae* infection levels were performed by determining the *P. sojae* biomass at 36 hpi, measured as the ratio of *P. sojae Actin* to soybean *Actin20* as determined by genomic DNA qPCR (8). Each experiment was repeated three times using a total of 18 hairy roots from three independent soybean cotyledons per biological replicate. For oospore abundance analysis, a *P. sojae* transformant derived from P6497 and constitutively expressing cytoplasmic red fluorescence protein (RFP) (21) was inoculated onto transgenic hairy roots and oospores were counted after 36 hpi.

In Vivo Protein–Protein Interaction Assays. To test for protein–protein interactions using Co-IP experiments, the putative interacting proteins were transiently coexpressed in *N. benthamiana*, and Co-IP was performed with total proteins extracted from *N. benthamiana* leaves at 36 h after agroinfiltration (29). Protein extraction and immunoblotting were performed as previously described. Proteins separated by SDS/PAGE were transferred to an Immobilon-PSQ polyvinylidene difluoride membrane (pretreated with methanol for 15 s; Millipore) using the Mini Trans-Blot apparatus (Bio-Rad) at 120 mA for 2 h. Equal protein transfer was monitored by staining the membranes with Ponceau S (Sigma–Aldrich). The following primary antibodies were used in this study: α-His (Abmart catalog no. M20001), α-HA (Abmart catalog no. M20003), and α-GFP (Abmart catalog no. M20004). The appropriate secondary antibody goat anti-mouse IRDye 800CW (Odyssey, catalog no. 926–32210) was applied and proteins were detected using an Odyssey (LI-COR) scanner with excitation at 700 and 800 nm. Protein-binding activity was calculated from the intensity of protein signals on the corresponding immunoblot membranes measured using ImageJ software (28). The relative binding activities of the proteins were normalized and calculated as previously described (8).

In Vitro Protein–Protein Interaction Assays. To assay interactions between purified proteins, recombinant PsXEG1-HA-His_6 was purified from *P. pastoris* or *P. sojae* while GmGIP1-GFP or GmAP5-GFP were expressed by transient expression in *N. benthamiana* and then collected onto anti-GFP beads. The PsXEG1 proteins were mixed with the beads carrying GmAP5 or GmGIP1 at a final concentration of 10 μM in equilibration buffer [50 mM Tris·HCl, pH 7.4, 150 mM NaCl, 1 mM EDTA, 1% Nonidet P-40, 0.5% sodium deoxycholate,

and 1× protease inhibitor mixture (Sigma)], then incubated for 1 h at 4 °C. Western blotting was then performed as described in section 14, above.

To measure protein binding by biolayer interferometer analysis, we used anti-Penta-HIS Dip and Read Biosensors (ForteBio) to measure the binding of PsXEG1 (produced in *P. pastoris*) and deglycosylated PsXEG1 to GmGIP1. Graded amounts of PsXEG1 and deglycosylated PsXEG1 were captured on an antibody-coated biosensor. GmGIP1 binding experiments were performed using an Octet QKe biolayer interferometer (ForteBio). The proteins were all diluted in PBS, pH = 7.4, 0.01% bovine serum albumin, and 0.002% Tween-20 (kinetic buffer).

Data Availability. Sequence data from this article can be found in the GenBank under the following accession numbers: PsXEG1 (EGZ16757.1), GmGIP1 (XP_003520561.1) and GmAP5 (XP_003538390.1). Accession numbers for GmAP5 and homologous genes from soybean (Williams 82) used in this article are listed in Dataset S1. RNA-seq data were obtained from NCBI SRA accession no. SRP073278. All other study data are included in the article and supporting information.

ACKNOWLEDGMENTS. We thank Prof. W. Ma (University of California, Riverside) and Prof. Renier A. L. van der Hoorn (University of Oxford) for insightful discussions and constructive suggestions, Prof. L. Liu (Nanjing Agricultural University) for glycobiology, Prof. K. Duan (Nanjing Agricultural University) for soybean genetic transformation, and Prof. Q. Yang (Dalian University of Technology) for protein expressed in *P. pastoris*. This research was supported by China National Funds for Innovative Research Groups Grant 31721004, the key program of National Natural Science Foundation of China Grant 31430073, Chinese Modern Agricultural Industry Technology System Grant CARS-004-PS14, and Fundamental Research Funds for the Central Universities Grant KYXK202010 (to Y. Wang). B.M.T. was supported by Oregon State University. Bioinformatic workstation was supported by the Bioinformatics Center, Nanjing Agricultural University.

1. T. Boller, S. Y. He, Innate immunity in plants: An arms race between pattern recognition receptors in plants and effectors in microbial pathogens. *Science* **324**, 742–744 (2009).
2. B. M. Tyler *et al*., *Phytophthora* genome sequences uncover evolutionary origins and mechanisms of pathogenesis. *Science* **313**, 1261–1266 (2006).
3. G. Doehlemann, C. Hemetsberger, Apoplastic immunity and its suppression by filamentous plant pathogens. *New Phytol.* **198**, 1001–1016 (2013).
4. Y. Wang, B. M. Tyler, Y. Wang, Defense and counterdefense during plant-pathogenic oomycete infection. *Annu. Rev. Microbiol.* **73**, 667–696 (2019).
5. P. N. Dodds, J. P. Rathjen, Plant immunity: Towards an integrated view of plant-pathogen interactions. *Nat. Rev. Genet.* **11**, 539–548 (2010).
6. B. M. Tyler, *Phytophthora sojae*: Root rot pathogen of soybean and model oomycete. *Mol. Plant Pathol.* **8**, 1–8 (2007).
7. Y. Wang *et al*., Leucine-rich repeat receptor-like gene screen reveals that *Nicotiana* RXEG1 regulates glycoside hydrolase 12 MAMP detection. *Nat. Commun.* **9**, 594 (2018).
8. Z. Ma *et al*., A paralogous decoy protects *Phytophthora sojae* apoplastic effector PsXEG1 from a host inhibitor. *Science* **355**, 710–714 (2017).
9. Z. Ma *et al*., A *Phytophthora sojae* glycoside hydrolase 12 protein is a major virulence factor during soybean infection and is recognized as a PAMP. *Plant Cell* **27**, 2057–2072 (2015).
10. T. Yoshizawa, T. Shimizu, H. Hirano, M. Sato, H. Hashimoto, Structural basis for inhibition of xyloglucan-specific endo-β-1,4-glucanase (XEG) by XEG-protein inhibitor. *J. Biol. Chem.* **287**, 18710–18716 (2012).
11. C. W. Li *et al*., Glycosylation and stabilization of programmed death ligand-1 suppresses T-cell activity. *Nat. Commun.* **7**, 12632 (2016).
12. P. Buscaill *et al*., Glycosidase and glycan polymorphism control hydrolytic release of immunogenic flagellin peptides. *Science* **364**, eaav0748 (2019).
13. Y. Fang, B. M. Tyler, Efficient disruption and replacement of an effector gene in the oomycete *Phytophthora sojae* using CRISPR/Cas9. *Mol. Plant Pathol.* **17**, 127–139 (2016).
14. Z. Dubrow *et al*., Tomato 14-3-3 proteins are required for Xv3 disease resistance and Interact with a subset of *Xanthomonas euvesicatoria* Effectors. *Mol. Plant Microbe Interact.* **31**, 1301–1311 (2018).
15. J. Tahir, M. Rashid, A. J. Afzal, Post-translational modifications in effectors and plant proteins involved in host–pathogen conflicts. *Plant Pathol.* **68**, 628–644 (2019).
16. X. L. Chen *et al*., N-glycosylation of effector proteins by an α-1,3-mannosyltransferase is required for the rice blast fungus to evade host innate immunity. *Plant Cell* **26**, 1360–1376 (2014).
17. Y. Xia, Proteases in pathogenesis and plant defence. *Cell. Microbiol.* **6**, 905–913 (2004).
18. R. A. van der Hoorn, Plant proteases: From phenotypes to molecular mechanisms. *Annu. Rev. Plant Biol.* **59**, 191–223 (2008).
19. M. Tian, B. Benedetti, S. Kamoun, A Second Kazal-like protease inhibitor from *Phytophthora infestans* inhibits and interacts with the apoplastic pathogenesis-related protease P69B of tomato. *Plant Physiol.* **138**, 1785–1793 (2005).
20. M. Tian *et al*., A *Phytophthora infestans* cystatin-like protein targets a novel tomato papain-like apoplastic protease. *Plant Physiol.* **143**, 364–377 (2007).
21. M. Jing *et al*., A *Phytophthora sojae* effector suppresses endoplasmic reticulum stress-mediated immunity by stabilizing plant Binding immunoglobulin Proteins. *Nat. Commun.* **7**, 11685 (2016).
22. D. Dou *et al*., RXLR-mediated entry of *Phytophthora sojae* effector Avr1b into soybean cells does not require pathogen-encoded machinery. *Plant Cell* **20**, 1930–1947 (2008).
23. A. Kereszt *et al*., Agrobacterium rhizogenes-mediated transformation of soybean to study root biology. *Nat. Protoc.* **2**, 948–952 (2007).
24. S. Subramanian, M. Y. Graham, O. Yu, T. L. Graham, RNA interference of soybean isoflavone synthase genes leads to silencing in tissues distal to the transformation site and to enhanced susceptibility to *Phytophthora sojae*. *Plant Physiol.* **137**, 1345–1353 (2005).
25. J. Wong *et al*., Roles of small RNAs in soybean defense against *Phytophthora sojae* infection. *Plant J.* **79**, 928–940 (2014).
26. Q. Wang *et al*., Transcriptional programming and functional interactions within the *Phytophthora sojae* RXLR effector repertoire. *Plant Cell* **23**, 2064–2086 (2011).
27. M. Shabab *et al*., Fungal effector protein AVR2 targets diversifying defense-related cys proteases of tomato. *Plant Cell* **20**, 1169–1183 (2008).
28. S. Dong *et al*., Effector specialization in a lineage of the Irish potato famine pathogen. *Science* **343**, 552–555 (2014).
29. J. Win, S. Kamoun, A. M. Jones, Purification of effector-target protein complexes via transient expression in *Nicotiana benthamiana*. *Methods Mol. Biol.* **712**, 181–194 (2011).